Thermodynamic stability conditions of clathrate hydrates for refrigerant (R134a or R410a or R507) with MgCl$_2$ aqueous solution

Peterson Thokozani Ngema [a], Paramespri Naidoo [a], Amir H. Mohammadi [a, b, c, *], Dominique Richon [a, d], Deresh Ramjugernath [a, **]

[a] Thermodynamics Research Unit, School of Engineering, University of KwaZulu-Natal, Howard College Campus, King George V Avenue, Durban 4041, South Africa
[b] Département de Génie des Mines, de la Métallurgie et des Matériaux, Faculté des Sciences et de Génie, Université Laval, Québec, (QC), G1V 0A6, Canada
[c] Institut de Recherche en Génie Chimique et Pétrolier (IRGCP), Paris Cedex, France
[d] Department of Biotechnology and Chemical Technology, School of Science and Technology, Aalto University, Aalto, Finland

ARTICLE INFO

ABSTRACT

Clathrate hydrate dissociation data were measured for systems comprising of refrigerants (R134a, R410a and R507) + water + MgCl$_2$ at varying salt concentrations. The ternary system for R134a + water + MgCl$_2$ was measured at salt concentrations of (0.259, 0.546, and 0.868) mol.kg^{-1} in the temperature range of (277.1–283) K and a pressure range of (0.114–0.428) MPa. Hydrate measurements for the {R410a or R507} + water + MgCl$_2$ systems were measured at salt concentrations of (0.259 and 0.546) mol.kg^{-1} in the temperature range of (274.3–293) K and a pressure range of (0.154–1.421) MPa. The isochoric pressure-search method was used to measure the hydrate dissociation data. This study is a continuation of previous investigations which focused on obtaining hydrate dissociation data for R134a, R410a and R507 refrigerants in NaCl and CaCl$_2$ aqueous solutions. The measured hydrate dissociation data can be used to design industrial wastewater treatment and desalination processes. The results show that the effect of salt concentration on hydrate formation is smaller for MgCl$_2$ aqueous solutions compared to CaCl$_2$ and NaCl as salt concentration increases. Modelling of the measured data is performed using a combination of the solid solution theory of van der Waals and Platteeuw, the Aasberg–Petersen et al. model, and the Peng–Robinson equation of state with classical mixing rules. The model is in good agreement with the measured hydrate dissociation data.

© 2015 Elsevier B.V. All rights reserved.

1. Introduction

Gas hydrate, or clathrate hydrate, formation has been recognised as a promising technology for concentrating aqueous solutions, in comparison to the common technologies which include evaporation or freeze crystallization, due to its reduced energy consumption. Gas hydrates are defined as solid crystalline structures, physically similar to ice, in which gas molecules are surrounded by hydrogen bonded water molecules (which form cages), at conditions of elevated temperature and high pressure [1–7].

* Corresponding author. Thermodynamics Research Unit, School of Engineering, University of KwaZulu-Natal, Howard College Campus, King George V Avenue, Durban 4041, South Africa.
** Corresponding author.
E-mail addresses: a.h.m@irgcp.fr, amir_h_mohammadi@yahoo.com (A.H. Mohammadi), ramjuger@ukzn.ac.za (D. Ramjugernath).

Generally, there are three typical hydrate crystalline structures with different cage sizes, shapes, and numbers of cavities or cages: structure I (sI), structure II (sII) and structure H (sH) [3]. The third type of structure which is termed structure H (sH) is less common [3]. Gas hydrate or clathrate hydrate technology has gained interest from researchers as a means for the production of potable water from industrial wastewater and seawater. Gas hydrates have been shown to have positive applications in wastewater treatment and desalination, CO$_2$ capture and separation, separation of close-boiling point compounds, hydrogen/methane storage, etc [1–6].

The chemical structure of gas hydrates allows for the gas molecule (refrigerant) to form hydrates with water only. Salts and other impurities are excluded from hydrate formation, leaving them in the residual saline water [6,8]. Fresh water is recovered as a final product when hydrate crystals dissociate. It has been shown that refrigerants can form clathrate hydrates at pressures below 2 MPa [3,4,8–19]. Refrigerants can play an important role in water

desalination or wastewater treatment [3,4,8–19]. To develop low cost desalination processes, a low pressure hydrate medium should be employed [18–22]. Javanmardi and Moshefeghian [4], Cha and Seol [8], Eslamimanesh et al. [9], Chun et al. [10], Petticrew [17], Ngema et al. [18], Ngema [19], and Seo and Lee [22] have reported that the use of refrigerants to form gas hydrate enables hydrate formation at near ambient conditions compared to hydrate formation using hydrocarbons. In addition, it was reported that gas hydrate technology is promising when compared to membrane desalination processes. Park et al. [7] investigated the potential application of gas hydrates for desalination processes by studying the elimination efficiencies for each dissolved mineral salt from seawater samples. The Inductively Coupled Plasma Atomic Emission Spectroscopy (ICP-AES) analyser was used to test dissolved mineral salts in seawater samples. Park et al. [7] showed that in a single stage hydrate process, 72–80% of each dissolved mineral (K^+, Na^+, Mg^{2+}, B^{3+} and Ca^{2+}) was removed. Chun et al. [10] measured the phase equilibrium data for the ternary system chloro(difluoro) methane (R22) + water + {NaCl, KCl, and $MgCl_2$} at varying electrolyte compositions. The phase equilibrium data were measured in a temperature range of (273.9–287.8) K and a pressure range of (0.140–0.790) MPa. It was noted that the addition of electrolytes to the aqueous solutions inhibit hydrate formation which shifts the dissociation data towards lower temperatures.

The generated hydrate dissociation data can be used for the design of wastewater treatment and desalination processes using gas hydrate technology. Petticrew [17], Ngema et al. [18], and Ngema [19] investigated the influence of NaCl and $CaCl_2$ aqueous solutions on R134a, R410a and R507 at varying salt concentrations. It was noted that the addition of NaCl and $CaCl_2$ to the {R134a or R507 or R410a} + water systems shifts the Hydrate–Liquid water–Vapor ($H–L_W–V$) phase boundary towards lower temperatures with increasing salt concentration. Furthermore, it was found that these systems exhibit a quadruple point, i.e. all four phases, Hydrate–Liquid water–Liquid refrigerant–Vapor ($H–L_W–L_{Refrigerant}–V$) coexist. The application of gas hydrates in desalination processes and saline water systems has been reported in several studies [1–19,23–50]. Many hydrate phase equilibrium studies have been done for hydrocarbon/CO_2/H_2S + salt (mainly NaCl) + water systems. A comprehensive review for the latter systems is given by Sloan and Koh [3] and NIST [50]. To the best of our knowledge, there is limited information for hydrate phase equilibrium in refrigerant + salt (especially $MgCl_2$) + water systems.

This study is a continuation of previous studies concerning the effects of NaCl and $CaCl_2$ on hydrate formation using R134a, R410a and R507 as hydrate formers. In this study, the effect of $MgCl_2$ aqueous solutions in fluorinated refrigerant hydrates is investigated. These refrigerant gases are environmentally friendly (low global warming potential) and are able to form hydrates at lower pressures than natural hydrate formers such as methane. These fluorinated refrigerants are available commercially and there is some hydrate studies reported in the literature [12,18,19] with pure water.

In this communication, the hydrate measurements were undertaken at varying concentrations of magnesium chloride in order to see the effect of salt in R134a, R507 and R410a. Measurements for the R134a + water + $MgCl_2$ system were undertaken at salt concentration of (0.259, 0.546, and 0.868) mol.kg^{-1}, while the {R410a or R507} + water + $MgCl_2$ systems were measured at salt concentration of (0.259 and 0.546) mol.kg^{-1}. Table 1 presents the range of conditions for the gas hydrate dissociation experiments. The experimental dissociation data were modelled using a combination of the Aasberg-Petersen et al. [51] model which describes the electrolyte aqueous system; the hydrate phase is described by the solid solution theory of van der Waals and Platteeuw [52]. The

Table 1
Molality, and temperature and pressure ranges studied for hydrate dissociation condition measurements (w_i = molality of salt in aqueous solution).

Hydrate former	Salt	w_i (mol.kg^{-1})	Temperature (K)	Pressure (MPa)
R410a	No salt	–	277.5 to 293.0	0.179 to 1.421
	$MgCl_2$	0.259	276.0 to 291.8	0.155 to 1.343
		0.546	274.9 to 291.0	0.154 to 1.292
R507	No salt	–	277.7 to 283.3	0.221 to 0.873
	$MgCl_2$	0.259	276.5 to 282.6	0.212 to 0.823
		0.546	274.3 to 280.9	0.174 to 0.769
R134a	No salt	–	277.1 to 283.0	0.114 to 0.428
	$MgCl_2$	0.259	277.1 to 282.3	0.131 to 0.410
		0.546	275.4 to 280.9	0.116 to 0.385
		0.868	274.7 to 278.9	0.135 to 0.356

Peng–Robinson [53] equation of state with classical mixing rules was used to describe the (non-electrolyte) aqueous/liquid and vapor phases. It should be noted that previous studies [9,11,15,17–19] have shown that R134a forms hydrates of type sII with large cavities. R134a, R410a and R507 have large molecules, which cannot enter the small cavities of their relevant gas hydrate structures. The authors have used the latter assumptions in developing the thermodynamic model. However, the structure of the refrigerants used need to be further investigated using physical techniques like Raman Spectroscopy, or X-Ray Diffraction.

2. Experimental

2.1. Materials

Table 2 presents the details of the suppliers of the chemicals, as well as the purities of the chemicals used in this study. The purities for R134a, R410a and R507 were checked using gas chromatography (Shimadzu 2010 gas chromatograph (GC) equipped with a thermal conductivity detector and a Porapak Q column). Ultrapure Mill-Q water (electrical resistivity of 18 MΩ cm at 298.15 K) was used in all the experiments. The gravimetric technique was used to prepare the $MgCl_2$ aqueous solutions. An analytical mass balance (Ohaus Adventurer balance, model No. AV 114) which was calibrated by the supplier with a stated uncertainty of ±0.0001 g in mass was used for the preparation of the aqueous solutions.

2.2. Apparatus

Fig. 1 shows a schematic diagram of the equilibrium cell and the apparatus used in this study. A full description of equilibrium cell is given by Ngema [19]. A platinum resistance thermometer (Pt-100) was used to measure the equilibrium temperatures. The Pt-100 temperature probe was calibrated using a bath with ethylene glycol and a WIKA primary temperature sensor which was connected to a WIKA CTH 6500 multimeter. The primary temperature sensor was calibrated by the supplier. It has an uncertainty of ±0.03 K. The resultant combined uncertainty for the reported temperature is ±0.1 K (k = 2). The equilibrium cell pressure was measured using a WIKA pressure transmitter which has a pressure maximum operating limit of 10 MPa. It was calibrated in the range of 0–10 MPa against a standard pressure transmitter from WIKA. The resultant combined uncertainty for the reported pressure is estimated to be ±0.005 MPa (k = 2).

2.3. Experimental method

The isochoric pressure search method [3,18,19,30] was used to undertake hydrate dissociation data measurements presented in this study. Deionized water was first used to clean the equilibrium

Table 2
Formula, molecular weights, purities, critical properties and acentric factors, and suppliers of refrigerant studied.

Chemicals	Formula	Molecular weight (g.mol^{-1})	Supplier	Purity* (mass fraction)	T_c (K)	P_c(MPa)	ω
Water	H_2O	18.015[a]	UKZN	1.000	647.14[a]	22.064[a]	0.344[a]
R507	$0.5CHF_2CF_3 + 0.5\ CH_3CF_3$[g]	98.80[b]	Afrox	0.998	343.96[b]	3.797[b]	0.304[f]
R134a	CF_3CH_2F	102.03[c]	Afrox	0.999	374.18[c]	4.057[c]	0.326[c]
R410a	$0.5CH_2F_2 + 0.5\ CHF_2CF_3$[g]	72.60[d]	Afrox	0.998	345.65[d]	4.964[d]	0.279[f]
Magnesium chloride	$MgCl_2$	95.21*	Merck	0.990			

*As stated by the supplier. Checked by GC analysis for the gases and liquids.
T_c represents the critical temperature.
P_c stands for the critical pressure.
ω is the acentric factor.
[a] Reference [63].
[b] Reference [54].
[c] Reference [55].
[d] Reference [57].
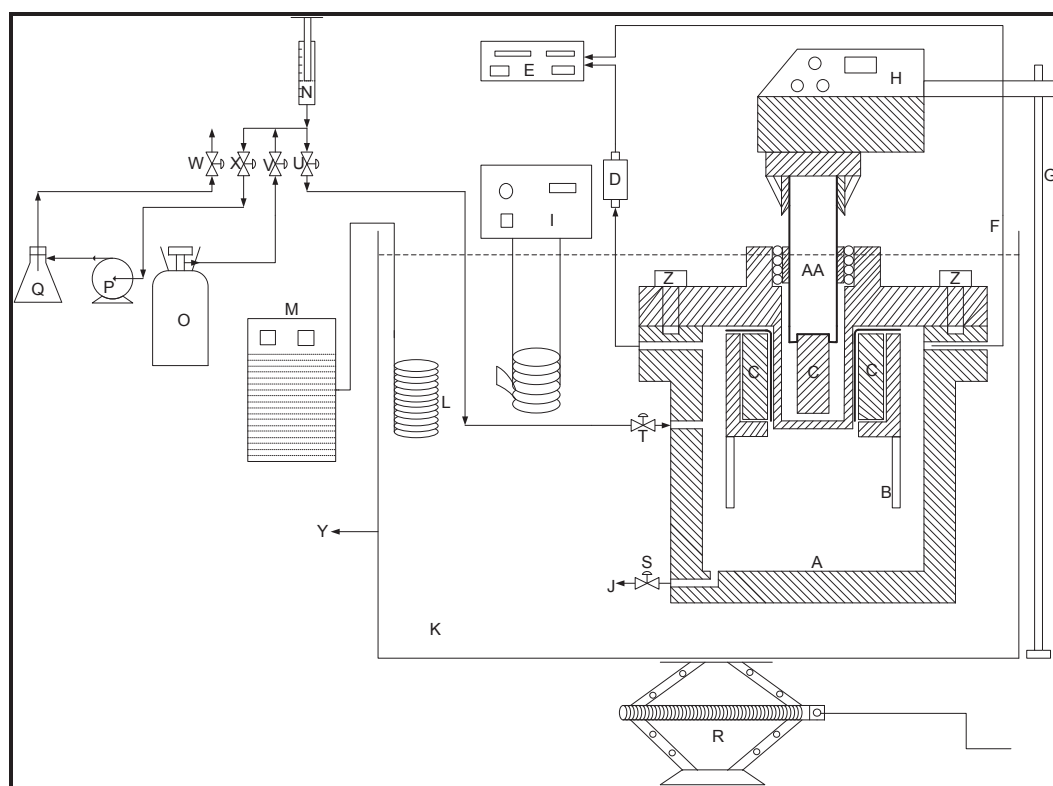[f] Reference [64].
[g] MASS fraction.

Fig. 1. Schematic diagram of the apparatus: A, Isochoric cell; B, Impeller; C, Neodymium magnet; D, Pressure transducer; E, Data acquisition unit; F, Pt-100; G, Stainless steel stand; H, Overhead mechanical stirrer; I, Temperature programmable circulator; J, Drain line; K, Chilling fluid; L, Cooling coil; M, Cold finger; N, Liquid syringe with aqueous solution; O, Refrigerant gas cylinder; P, Vacuum pump; Q, Vacuum flask; R, Mechanical jack; S, Drain valve; T, Inlet valve; U, Loading valve; V, Gas valve, W, Vent valve to atmosphere; X, Vacuum valve; Y, Water bath and Z, Stainless steel bolts; AA, Mechanical shaft.

cell. Thereafter, acetone was used to rinse the equilibrium cell. The acetone residual was then drained. The cell was evacuated to a pressure of 0.2 kPa for a period of 30 min at a constant temperature of 313.15 K to ensure that there were no traces of impurities. Approximately 15 cm³ of $MgCl_2$ aqueous solution was charged into the cell. The mechanical jack was used to raise the bath until the equilibrium cell is covered by the bath solution. Refrigerant was charged into the equilibrium cell through a pressure regulating valve. The cell contents were then stirred to ensure homogenous mixing and to allow refrigerant absorption into the solution until stabilization of the temperature and pressure.

Prior to the formation of the gas hydrate, the temperature and pressure are stable outside the hydrate formation region. The system temperature was then slowly decreased to facilitate the formation of gas hydrates. During this stage, the pressure decreases linearly with the system temperature. The point at which a rapid pressure drop is observed indicates the formation of gas hydrate. Thereafter the hydrate crystals are dissociated by gradually increasing the system temperature. As the dissociation point is approached, the incremental step in system temperature is set to 0.1 K. The time taken to reach equilibrium for each system temperature increment of 0.1 K was approximately one hour. Fig. 2 shows a pressure–temperature plot indicative of the isochoric pressure search method for the formation and dissociation of hydrate crystals. The hydrate former is released at the point where the cooling curve and heating curve intersect. Finally, the system goes
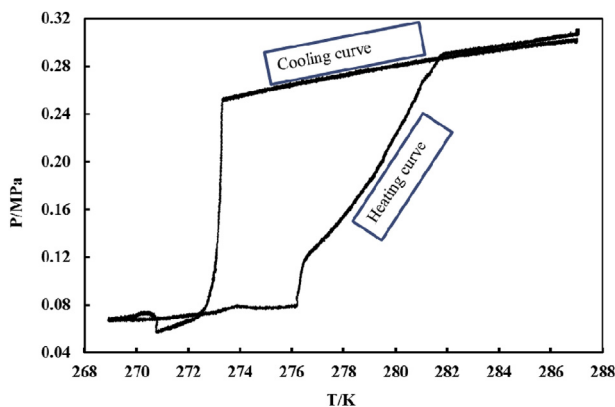
Fig. 2. Typical hydrate formation and dissociation curves for the R134a (1) + water (2) system.

back to the initial conditions which are outside the hydrate formation region. Consequently, the point of intersection of the cooling and heating curves is called the gas hydrate dissociation point where system temperature and pressure are at equilibrium.

3. Thermodynamic model

The modelling of the measured hydrate dissociation data was undertaken using a combination of the Aasberg-Petersen et al. [51] model which describes the electrolyte aqueous system, with the hydrate phase described by the solid solution theory of van der Waals and Platteeuw [52]. The Peng—Robinson [53] equation of state with classical mixing rules was used to describe the (non-electrolyte) aqueous/liquid and vapor phases. These models are described in detail by Ngema et al. [18] and Ngema [19]. The solid solution theory of the van der Waals and Platteeuw [52] model was modified by Parrish and Prausnitz [61]. Later this model was adapted by Eslamimanesh et al. [9]. In this study, the modified model of Eslamimanesh et al. [9] was used to model the hydrate phase using the computational algorithm (flow diagram) as presented by Petticrew [17]. In addition, the electrolyte model of Aasberg-Petersen et al. [51] which was modified by Tohidi et al. [62] was used in this study.

4. Results and discussion

The vapor pressures of {R410a or R134a or R507} were measured by Ngema et al. [18] and Ngema [19] to validate the sensor calibrations and operating procedure for the equilibrium cell and they were compared against the available literature [54—56] data. Ngema [19] measured the binary test systems for {R410a or R134a} + water and compared the data to literature [10,12,15—17]. These two binary systems were studied to verify the reliability of the equipment and the isochoric pressure-search method to obtain reliable gas hydrate phase equilibrium data.

The gas hydrate dissociation data for the {R134a or R507 or R410a} + water + MgCl2 systems are presented in Tables 3—5 and illustrated in Figs. 3—5. According to Eslamimanesh et al. [9], it is expected that when the gas hydrate dissociates, pure/clean water is produced for the proposed desalination process. However, there can be very small amounts of salt present in the hydrate phase. Thereafter, the refrigerant is released, and it can be used to form more hydrate [3,4,6,10,18,19]. The {R507 or R410a or R134a} + water + MgCl2 systems exhibit a quadruple point where four phases (H—Lw—Lrefrigerant—V) coexist. Previous studies by

Table 3
Experimental dissociation conditions of gas hydrates for the R134a (1) + water (2) + MgCl2 (3) system at various concentrations of Salt.[a,b]

R134a (1) + water (2)		R134a (1) + water (2) + 0.259 mol kg^{-1} MgCl2 (3)		R134a (1) + water (2) + 0.546 mol kg^{-1} MgCl2 (3)	
T (K)	P (MPa)	T (K)	P (MPa)	T (K)	P (MPa)
283.0	0.428	282.3	0.410	280.9	0.385
282.8	0.400	281.9	0.372	280.6	0.365
282.4	0.368	281.4	0.335	280.3	0.338
282.2	0.350	280.9	0.296	279.9	0.313
281.6	0.308	280.3	0.256	279.5	0.286
281.0	0.269	279.6	0.224	278.7	0.247
280.5	0.236	278.4	0.173	277.9	0.205
279.2	0.180	277.8	0.151	277.3	0.178
278.4	0.150	277.1	0.131	276.6	0.153
277.1	0.114			275.4	0.116

R134a (1) + water (2) + 0.868 mol kg^{-1} MgCl2 (3)

278.9	0.356
278.3	0.317
277.9	0.287
277.5	0.260
276.9	0.226
276.2	0.198
275.7	0.175
274.7	0.135

[a] $U(T) = \pm 0.1$ K, k = 2.
[b] $U(P) = \pm 0.005$ MPa, k = 2.

Table 4
Experimental dissociation conditions of gas hydrates for the R507 (1) + water (2) + MgCl2 (3) system at various concentrations of Salt.[a,b]

R507 (1) + water (2)		R507 (1) + water (2) + 0.259 mol kg^{-1} MgCl2 (3)		R507 (1) + water (2) + 0.546 mol kg^{-1} MgCl2 (3)	
T (K)	P (MPa)	T (K)	P (MPa)	T (K)	P (MPa)
283.3	0.873	282.6	0.823	280.9	0.769
283.0	0.740	282.2	0.756	280.5	0.714
282.2	0.611	281.6	0.651	279.6	0.579
281.3	0.504	281.0	0.563	278.8	0.505
280.7	0.444	280.0	0.462	278.0	0.425
280.0	0.370	279.1	0.379	277.2	0.353
279.0	0.297	278.4	0.319	276.2	0.279
278.1	0.241	277.5	0.264	275.4	0.231
277.7	0.221	276.5	0.212	274.3	0.174

[a] $U(T) = \pm 0.1$ K, k = 2.
[b] $U(P) = \pm 0.005$ MPa, k = 2.

Ngema et al. [18] and Ngema [19] indicate that a water insoluble promoter (cyclopentane or cyclohexane) is required for the {R507 or R134a} + water + {NaCl or CaCl2} systems. In this study, the water insoluble promoter (cyclopentane or cyclohexane) is required for the {R507 or R134a} + water + MgCl2 systems because their dissociation temperatures are lower than ambient temperature. Furthermore, it should be noted that the R410a + water + MgCl2 system forms hydrates at conditions close to ambient temperatures.

Experimental results show that the addition of MgCl2 causes the phase equilibrium boundary to shift significantly towards lower dissociation temperatures as salt concentration increases. However, MgCl2 shows a low inhibition effect on the R410a + water + MgCl2 system compared to the {R507 or R134a} + water + MgCl2 systems, as illustrated in Figs. 3—5.

The systems measured are modelled using a combination of the Aasberg-Petersen et al. [51] model which describes the electrolyte aqueous system, with the hydrate phase described by the solid solution theory of van der Waals and Platteeuw [52]. The

Table 5
Experimental dissociation conditions of gas hydrates for the R410a (1) + water (2) + MgCl$_2$ (3) system at various concentrations of Salt.[a,b]

R410a (1) + water (2)		R410a (1) + water (2) + 0.259 mol kg^{-1} MgCl$_2$ (3)		R410a (1) + water (2) + 0.546 mol kg^{-1} MgCl$_2$ (3)	
T (K)	P (MPa)	T (K)	P (MPa)	T (K)	P (MPa)
293.0	1.421	291.8	1.343	291.0	1.292
291.3	1.185	291.5	1.290	289.9	1.122
290.3	1.034	290.5	1.118	288.7	0.983
289.0	0.868	289.3	0.946	287.2	0.811
287.8	0.741	288.0	0.789	285.7	0.668
286.0	0.582	286.3	0.641	284.2	0.548
284.6	0.484	284.6	0.510	282.7	0.446
283.1	0.396	283.3	0.419	281.0	0.357
280.3	0.257	281.9	0.350	278.7	0.270
277.5	0.179	280.1	0.274	276.9	0.201
		278.2	0.217	274.9	0.154
		276.0	0.155		

[a] $U(T) = \pm 0.1$ K, k = 2.
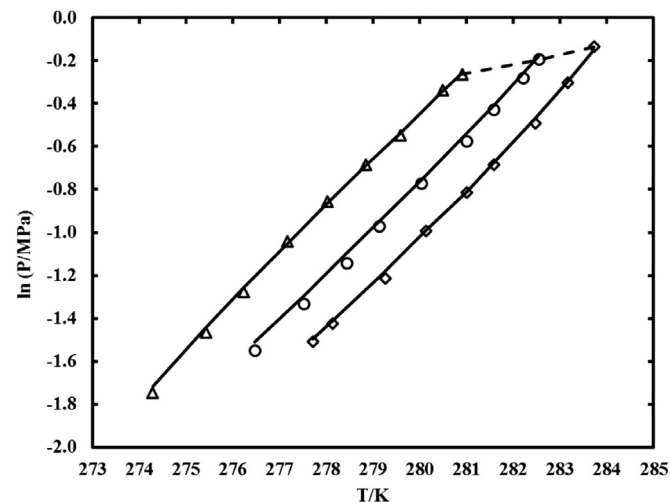[b] $U(P) = \pm 0.005$ MPa, k = 2.

Fig. 4. Experimental and calculated hydrate dissociation conditions for the R410a (1) + Water (2) + MgCl$_2$ (3) System. . Symbols represent experimental data. Solid lines show model results: This work: ◇, No Salt; ○, 0.259 mol kg^{-1}; Δ, 0.546 mol kg^{-1}; − −, Quadruple Point Line.

Fig. 3. Experimental and calculated hydrate dissociation conditions for the R507 (1) + Water (2) + MgCl$_2$ (3) System. Symbols represent experimental data. Solid lines show model results: This work: ◇, No Salt; ○, 0.259 mol kg^{-1}; Δ, 0.546 mol kg^{-1}; − −, Quadruple Point Line.

Fig. 5. Experimental and calculated hydrate dissociation conditions for the R134a (1) + Water (2) + MgCl$_2$ (3) System. Symbols represent experimental data. Solid lines show model results: This work: ◇, No Salt; ○, 0.259 mol kg^{-1}; Δ, 0.546 mol kg^{-1}; □, 0.868 mol kg^{-1}; − −, Quadruple Point Line.

Peng–Robinson [53] equation of state with classical mixing rules was used to describe the (non-electrolyte) aqueous/liquid and vapor phases. The model for the electrolyte system assumes that in the vapor phase there are no ions present and the salt does not enter the hydrate phase.

Table 6 presents the Langmuir constant parameters (c and d) which were obtained using Eq. (1), in the absence of salt. In this study, the model parameters for the Langmuir constants for the hydrate former interaction with each type of cavity has been calculated using Eq. (1) for a large cavity (tetrakaidecahedra (sI) and hexakaidecahedra (sII)) [9,18,19,60,61].

$$C_{large} = \frac{c}{T} \exp\left(\frac{d}{T}\right) \qquad (1)$$

where T is in K and C has units of reciprocal MPa.

Sloan and Koh [3], Eslamimanesh et al. [9], Petticrew [17], Ngema et al. [18], Ngema [19], Mohammadi et al. [58], and Mohammadi and Richon [59], used the following values for structure II of the gas hydrate $\nu'_{small} = 2/17$ and $\nu'_{large} = 1/17$ for the
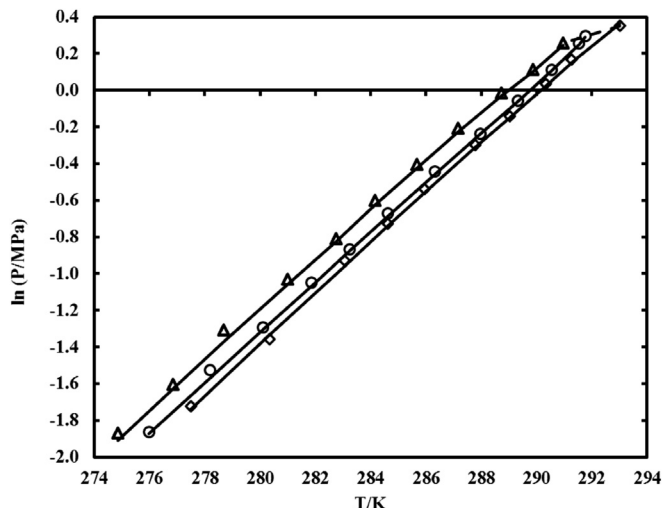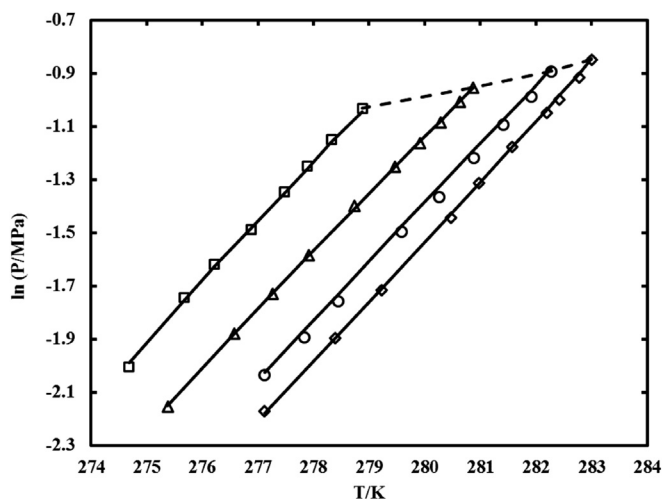
Table 6
Regressed Langmuir constants parameters for refrigerant gas hydrates.

Hydrate former	c (K.MPa^{-1})	d (K)	AAD[a]
R134a	5.70×10^{-3}	4908.71	5.30
R410a	4.75×10^{-3}	5969.68	0.79
R507	4.50×10^{-4}	6233.08	0.83

P_i^{cal}: Calculated hydrate dissociation pressure.
P_i^{Exp}: Experimental hydrate dissociation pressure.
N: Number of data.

[a] $AAD(\%) = \frac{100}{N} \sum_i^N \frac{|P_i^{Cal} - P_i^{Exp}|}{P_i^{Exp}}$

number of cavities of type i per water molecule in the unit hydrate cell (ν'_i). The optimum values of the constants c and d are calculated by fitting the thermodynamic model to the measured hydrate dissociation data. Subsequently, the constants were regressed to adjust the parameters to dissociation data in the presence of MgCl$_2$

Table 7
Constants for Eq. 2

	A	B	C	D	E
MgCl₂[a]	−6.420*10^{00}	1.066*10^{-02}	−6.186*10^{-01}	−4.556*10^{-03}	−1.312*10^{-03}

[a] Reference [62].

aqueous solutions using constants listed in Table 7. For more details refer to Ngema et al. [18] and Ngema [19]. Aasberg-Peterson et al. [51] and Tohidi et al. [62] used Eq. (2) to undertake calculations for a number of water-electrolyte and gas-electrolyte systems.

$$h_{is} = \frac{A + BT + Cx + Dx^2 + ETx}{1000}$$ (2)

where h_{is} is an interaction coefficient between the dissolved salt and a non-electrolytic component. A, B, C, D and E are constants which are listed in Table 7, x is mole fraction, and T is temperature in K. By using the model combination, it was shown that the model provides a satisfactorily representation of the experimental hydrate dissociation data. It should be noted from Table 6 that the Langmuir constants and average absolute deviation (AAD) for the R134a + water system compare favourably with that of Eslamimanesh et al. [9].

5. Conclusions

Gas hydrate dissociation conditions for {R410a or R507 or R134a} + water + MgCl₂ systems were measured at varying salt concentration. It was observed that hydrate dissociation data for R507 and R134a are not suitable for desalination processes near ambient conditions. In this case, a water insoluble promoter (cyclopentane or cyclohexane) is recommended to be added in the {R507 or R134a} + water + MgCl₂ systems, which can shift the H−L$_W$−V equilibrium phase boundary closer to ambient conditions. It was observed that the influence of MgCl₂ aqueous solutions is less significant compared to NaCl as salt concentration increases. The results show that the MgCl₂ salt has an inhibition effect on the hydrate formation, in which the H−L$_W$−V equilibrium phase boundary is shifted towards lower temperatures. Experimental dissociation data were correlated using a combination of the Aasberg-Petersen et al. [51] model which describes the electrolyte aqueous system, the hydrate phase is described by the solid solution theory of van der Waals and Platteeuw [52]. The Peng−Robinson [53] equation of state with classical mixing rules was used to describe the (non-electrolyte) aqueous/liquid and vapor phases.

Acknowledgements

References

[1] A.H. Mohammadi, D. Richon, Ind. Eng. Chem. Res. 49 (2010) 925−928.
[2] K. Tumba, P. Reddy, P. Naidoo, D. Ramjugernath, A. Eslamimanesh, A.H. Mohammadi, D. Richon, J. Chem. Eng. Data 56 (2011) 3620−3629.
[3] E.D. Sloan, C.A. Koh, Clathrate Hydrates of Natural Gases, third ed., CRC Press, Taylor & Francis Group, London, New York, 2008.
[4] J. Javanmardi, M. Moshefeghian, Appl. Thermodyn. Eng. 23 (2003) 845−857.
[5] C.P. Huang, O. Fennema, W.D. Poweri, Cryobiology 2 (1966) 240−245.
[6] A. Eslamimanesh, A.H. Mohammadi, D. Richon, P. Naidoo, D. Ramjugernath, J. Chem. Thermodyn. 46 (2012) 62−71.
[7] K. Park, S.Y. Hong, J.W. Lee, K.C. Kang, Y.C. Lee, M.-G. Ha, J.D. Lee, Desalination 274 (2011) 91−96.
[8] J.-H. Cha, Y. Seol, Sustain. Chem. Eng. 1 (2013) 1218−1224.
[9] A. Eslamimanesh, A.H. Mohammadi, D. Richon, Chem. Eng. Sci. 66 (2011) 5439−5445.
[10] M.-K. Chun, H. Lee, B.J. Ryu, J. Chem. Eng. Data 45 (2000) 1150−1153.
[11] D. Liang, K. Guo, R. Wang, S. Fan, Fluid Phase Equilib. 187−188 (2001) 61−70.
[12] T. Akiya, T. Shimazaki, M. Oowa, M. Matsuo, Y. Yoshida, Int. J. Thermophys. 20 (1999) 1753−1763.
[13] Y. Seo, H. Tajima, A. Yamasaki, S. Takeya, T. Ebinuma, F. Kiyono, Environ. Sci. Technol. 38 (2004) 4635−4639.
[14] K. Maeda, Y. Katsura, Y. Asakuma, K. Fukui, Chem. Eng. Process 47 (2008) 2281−2286.
[15] A.H. Mohammadi, D. Richon, AIChE Annual Meeting, Proceeding, Salt Lake City, UT, 2010.
[16] S. Hashimoto, H. Miyauchi, Y. Inoue, K. Ohgaki, J. Chem. Eng. Data 55 (2010) 2764−2768.
[17] C. Petticrew, MSc Thesis in Chemical Engineering, University of KwaZulu-Natal, Durban, South Africa, 2011.
[18] P.T. Ngema, C. Petticrew, P. Naidoo, A.H. Mohammadi, D. Ramjugernath, J. Chem. Eng. Data 59 (2) (2014) 466−475.
[19] P.T. Ngema, MSc Thesis in Chemical Engineering, University of KwaZulu-Natal, Durban, South Africa, 2014.
[20] K.-H. Guo, B.-F. Shu, Z.-X. Meng, L. Zeng, Chinese Patent No. ZL95107268.4, 1995.
[21] K.-H. Guo, B.-F. Shu, W.-J. Yang, in: Proceedings of 1st Trabzon Int. Energy and Environment Symposium, Trabzon, Turkey 1, 1996, pp. 381−386.
[22] Y. Seo, H. Lee, Environ. Sci. Technol. 35 (2001) 3386−3390.
[23] A.J. McCormack, G.A. Niblock, Water Treatment Technology Program Report No. 31, Thermal Energy Storage, Inc., San Diege, CA, 1998.
[24] J.-H. Cha, Y. Seol, Sustain. Chem. Eng. 1 (2013) 1218−1224.
[25] R.W. Bradshaw, J.A. Greathouse, R.T. Cygan, B.A. Simmons, D.E. Dedrick, E.H. Majzoub, Sandia National Laboratories, Albuquerque, NM, Livermore, 2008.
[26] R. Rautenbach, A. Seide, Proceeding of International Symposium on Fresh Water from Sea, 1978, pp. 43−51.
[27] A.J. Barduhn, H.E. Towlson, Y.C. Hu, AIChE J. 8 (1962) 176−183.
[28] J. Sugi, S. Saito, Desalination 3 (1967) 27−31.
[29] S.L. Colten, F.S. Lin, T.C. Tsao, S.A. Stern, A.J. Barduhn, Desalination 11 (1972) 31−59.
[30] A.J. Barduhn, W.-C. Lee, Desalination 25 (1978) 151−162.
[31] R.A. McCormark, R.K. Andersen, Water Treatment Technology Program Report No. 5, Thermal Energy Storage, Inc, California, 1995.
[32] Y.T. Ngan, P. Englezos, Ind. Eng. Chem. Res. 35 (1996) 1894−1900.
[33] T. Younos, K.E. Tulou, J. Contemp. Water Res. Edu. 132 (2005) 3−10.
[34] M. Sarshar, A.H. Sharafi, 1st International Conference on Water and Wastewater Treatment, 2010, pp. 21−22. Isfahan, Iran.
[35] A.M. Aliev, R.Y. Yusifov, A.Z. Tairov, A.A. Sarydzhanoz, R.Y. Mirzoeva, Y.G. Yusifov, Theor. Found. Chem. Eng. 45 (2011) 185−189.
[36] M. Cakmakci, N. Kayaalp, I. Koyuncu, Desalination 222 (2008) 176−186.
[37] M.A. Clarke, A. Majumdar, P.R. Bishnoi, J. Chem. Eng. Data 49 (2004) 1436−1439.
[38] S.-P. Kang, M.-K. Chun, H. Lee, Fluid Phase Equilib. 147 (1998) 229−238.
[39] H. Kubota, K. Shimizu, Y. Tanaka, T. Makita, J. Chem. Eng. Jap. 17 (1984) 423−429.
[40] A.H. Mohammadi, D. Richon, J. Chem. Eng. Data 54 (2009) 2338−2340.
[41] A.H. Mohammadi, D. Richon, J. Chem. Thermodyn. 41 (2009) 1374−1377.
[42] J.J. Carroll, Natural Gas Hydrates: a Guide for Engineers, Gulf Professional Publishing, 2003. London New York Oxford.
[43] Z. Atik, C. Windmeier, L.R. Oellrich, J. Chem. Eng. Data 51 (2006) 1862−1867.
[44] P. Englezos, P.R. Bishnoi, Ind. Eng. Chem. Res. 30 (1991) 1655−1659.
[45] P. Englezos, Y.T. Ngan, J. Chem. Eng. Data 38 (1993) 250−253.
[46] M. Kharrat, D. Dalmazzone, J. Chem. Thermodyn. 35 (2003) 1489−1505.
[47] M.D. Jager, E.D. Sloan, Fluid Phase Equilib. 185 (2001) 89−99.
[48] A.H. Mohammadi, W. Afzal, D. Richon, J. Chem. Thermodyn. 40 (2008) 1693−1697.
[49] B. Tohidi, A. Danesh, A.C. Todd, IChemE 73 (1995) 464−472.
[50] NIST Data Gateway Database, http://www.nist.gov/gashydrate/system/salt.
[51] K. Aasberg-Petersen, E. Stenby, A. Fredenslund, Ind. Eng. Chem. Res. 30 (1991) 2180−2185.
[52] J.H. van der Waals, J.C. Platteeuw, Adv. Chem. Phys. 2 (1959) 1−57.
[53] D.Y. Peng, D.B. Robinson, Ind. Eng. Chem. Fundam. 15 (1976) 59−64.
[54] R. Döring, H. Buchwald, J. Hellmann, Int. J. Refrig 20 (2) (1997) 78−84.
[55] Aspen Plus Version V7.3, Aspen Technology Inc, 2011.
[56] J.E. Calm, Refrig. Manag. Serv. (2008) 1−14.

[57] W. Afzal, A.H. Mohammadi, D. Richon, J. Chem. Eng. Data 53 (2008) 663—666.
[58] A.H. Mohammadi, W. Afzal, D. Richon, J. Chem. Thermodyn. 40 (2008) 1693—1697.
[59] A.H. Mohammadi, D. Richon, J. Thermodyn. (2009) 1—12.
[60] P.B. Dharmawardhana, W.R. Parrish, E.D. Sloan, Ind. Eng. Chem. Fundam. 19 (4) (1980) 410—414.
[61] W.R. Parrish, J.M. Prausnitz, Ind. Eng. Chem. Process Des. Dev. 11 (1) (1972) 26—35.
[62] B. Tohidi, A. Danesh, A.C. Todd, Trans. IChemE 73 (1995) 464—472.
[63] B.E. Poling, J.M. Prausnitz, J.P. O'Connell, The Properties of Gases and Liquids, fifth ed., McGraw-Hill, New York, 2001.
[64] Y.I. Shouzhi, J.I.A. Yuanyuan, M.A. Peisheng, Chin. J. Chem. Eng. 13 (5) (2005) 709—712.